# Experimental Demonstration of Nonlinearity and Dispersion Compensation in an Embedded Link by Optical Phase Conjugation

Paolo Minzioni, Ilaria Cristiani, *Member, IEEE*, Vittorio Degiorgio, Lucia Marazzi, Mario Martinelli, Carsten Langrock, *Student Member, IEEE*, and M. M. Fejer, *Member, IEEE*

***Abstract*—We report in this letter, the experimental demonstration of simultaneous dispersion and nonlinearity compensation in an embedded link characterized by strongly asymmetrical power profiles. This result is obtained by using a highly efficient optical phase conjugator based on a periodically poled lithium-niobate waveguide, combined with two small dispersion-compensating elements properly inserted in the link.**

***Index Terms*—Nonlinear wave propagation, optical fiber communication, optical Kerr effect, optical phase conjugation.**

## I. Introduction

ONE OF the main transmission impairments in communication systems based on high bit-rate (>20 Gb/s) amplitude modulation, or on phase modulation at lower bit rates (∼10 Gb/s), is the signal distortion caused by the interplay between fiber chromatic dispersion and nonlinearity [1], [2]. Recently, much attention has been paid to compensation techniques based on the spectral inversion, which can be obtained through an optical phase conjugator (OPC) [3]–[5]. One of the most promising techniques is midspan spectral-inversion (MSSI) [6], [7], which allows for simultaneous compensation of the signal group velocity dispersion (GVD) [6] and the nonlinear effects [7], thus improving system performance. Unfortunately, the MSSI technique is effective only in systems exhibiting a symmetrical distribution of GVD and nonlinearity (and, thus, optical power) with respect to the center of the transmission link. Due to the presence of fiber losses, this "perfect symmetry" cannot be obtained in common transmission systems. As a consequence, the nonlinearity-compensation through MSSI has been demonstrated only in specifically designed links, in which customized dispersion maps [3], [5] or structures like short amplifier spacing [8], dispersion decreasing fibers [9], or high-power Raman distributed amplification [10] were used. An alternative solution proposed in [11] requires placement of the OPC at a specific position along the fiber cable, which might not be easily accessible in real systems.

In this letter, we experimentally demonstrate a highly effective single-channel nonlinearity compensation of an embedded link, characterized by strongly asymmetrical power profiles that make the MSSI technique not suitable. The employed configuration has been recently identified by theoretical investigations [12], [13] and a first description of its experimental implementation is reported in [14]. It is implemented by adding an OPC and two tailored dispersive elements at amplifier sites, without requiring either new access points to the cable, or the use of other complex structures. A significant improvement is found with respect to the MSSI technique. An important advantage of our compensation scheme is that it can be used to upgrade very simple links not including in-line dispersion compensators. Section II of this letter briefly explains the nonlinearity-compensation strategy. The experimental setup is described in Section III, and the obtained results are reported and discussed in Section IV.

## II. Theory

Nonlinearity-compensation techniques based on the use of an OPC, as well as those based on the use of a proper dispersion map, can be viewed as different strategies to satisfy a single requirement: the "highly nonlinear" regions (i.e., the regions of the link in which the pulse energy is higher) must be symmetrically distributed when plotted on a power versus accumulated dispersion diagram (PADD) [12]. This condition physically means that the effect of nonlinearity experienced by pulses during propagation through a "nonlinear region" depends on their accumulated GVD. In order to cancel out the accumulated nonlinear effects, pulses must also propagate through a complementary nonlinear region of the link, after having accumulated an opposite amount of GVD. Since pulses with an opposite value of accumulated dispersion can be seen as "temporally inverted," this requirement can be identified as a midnonlinearity-temporal-inversion (MNTI) condition, a generalized version of MSSI [12]. The MNTI configuration described here is obtained starting from a standard MSSI setup and inserting a dispersion compensating module (DCM) before the OPC, positioned at an amplifier site, as shown in Fig. 1.

The effect of the DCM is that of modifying the value of accumulated dispersion exhibited by the pulses during propagation along the nonlinear regions downstream of the OPC, as can be

Manuscript received December 5, 2005; revised February 13, 2006.

P. Minzioni, I. Cristiani, and V. Degiorgio are with CNISM and University of Pavia, Pavia 27100, Italy (e-mail: paolo.minzioni@unipv.it; ilaria.cristiani@unipv.it; vittorio.degiorgio@unipv.it).

L. Marazzi is with CoreCom, Milan 20133, Italy (e-mail: marazzi@corecom.it).

M. Martinelli is with CoreCom, Milan 20133, Italy, and also with Politecnico di Milano, Milan 20133, Italy (e-mail: martinel@elet.polimi.it).

C. Langrock and M. M. Fejer are with the Edward Ginzton Laboratory, Stanford University, Stanford, CA 94305 USA (e-mail: langrock@stanford.edu; fejer@stanford.edu).

Digital Object Identifier 10.1109/LPT.2006.873547

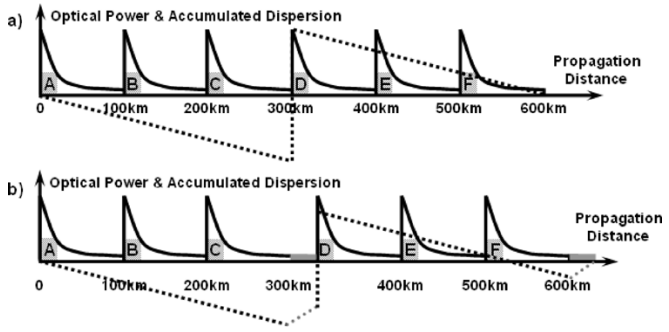


Fig. 1. Solid and dotted lines represent the power profiles and the GVD accumulated by pulses during propagation in the (a) MSSI and (b) MNTI configuration. In (b), the horizontal thick gray lines after 300 and 600 km of propagation correspond to the DCMs.

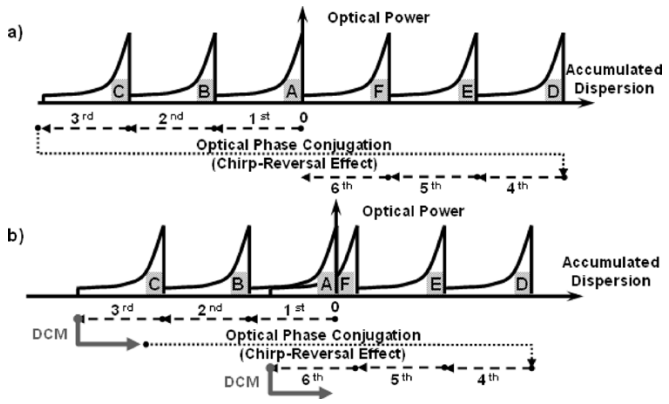


Fig. 2. PADDs given by the (a) MSSI and (b) MNTI configurations. Arrows indicate the propagation history of pulses along the spans ($1^{\mathrm{st}}, 2^{\mathrm{nd}}, \ldots, 6^{\mathrm{th}}$).

graphically observed comparing Fig. 1(a) and (b). In the MNTI configuration, an additional DCM with the same characteristics must be inserted at the end of the link to compensate the GVD added by the first DCM.

By plotting the power profiles of the two configurations in a PADD, one can easily notice that in MSSI [Fig. 2(a)] the distribution of the nonlinear regions (indicated in gray) is asymmetrical with respect to the zero value of accumulated GVD. Conversely, in MNTI [Fig. 2(b)], a perfect symmetry is obtained just by adding the appropriate DCM to compensate the dispersion accumulated by the pulses during the propagation in the linear region just before the OPC (third span in the figures). As demonstrated in [13], the optimum value of dispersion to be compensated before the OPC is given by $D{\cdot}(L_{\mathrm{amp}} - 1/\alpha)$, where $D$ is the fiber link dispersion, $L_{\mathrm{amp}}$ is the amplifier spacing, and $\alpha$ the fiber attenuation coefficient.

## III. Experimental Setup

The experimental setup is composed of three elements: the transmission terminals (transmitter and receiver), the fiber-optic system (fiber, amplifiers), and the OPC.

### A. Transmitter and Receiver

The transmitter used for the experiment is obtained by cascading two Mach–Zehnder lithium-niobate modulators, that produce a 10-Gb/s stream of return-to-zero pulses with a $T_{\mathrm{FWHM}} = 45$ ps. A $2^{31} - 1$ pseudorandom bit sequence is used to modulate the signal. At the receiver, the signal is amplified by a low-noise preamplifier and filtered for amplified spontaneous emission removal (filter bandwidth $\approx$ 1 nm). Subsequently, the signal power is modified by a variable attenuator, and the signal is then sent to a 99/1 splitter used to monitor its power (1% port) while sending the 99% to a PIN photodiode (connected to the bit-error-rate (BER) tester). This scheme allowed us to perform the BER measurements as a function of the optical power input to the photodiode.

TABLE I
Average Values of Main Fiber Parameters

| | $D$ [ps nm$^{-1}$ km$^{-1}$] | $D_2$ [ps nm$^{-2}$ km$^{-1}$] | $A_{eff}$ [$\mu$m$^2$] | $\alpha$ [dB km$^{-1}$] |
|---|---|---|---|---|
| NZDSF | -2.9 | 0.067 | 55 | 0.22 |
| SMF | + 16 | 0.072 | 82 | 0.23 |

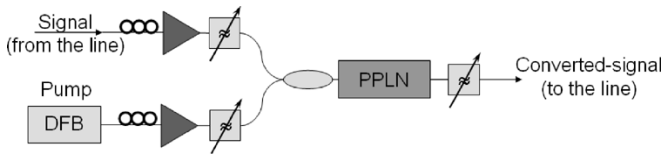


Fig. 3. Experimental setup for the OPC implementation.

### B. Transmission Line

The transmission line is composed of six spans of nonzero dispersion-shifted-fiber [(NZDSF) ITU G.655] exhibiting normal dispersion, with no in-line (distributed) dispersion compensation. Lumped erbium-doped fiber amplifiers are used to compensate for fiber losses. To realize the MNTI configuration [Fig. 1(b)], two spools of single-mode fiber [(SMF) ITU G.652] have been used as DCMs, one immediately before the OPC and the other at the receiver. Complete dispersion compensation was obtained in both configurations (residual dispersion $< 5$ ps nm$^{-1}$). The dispersion ($D$), dispersion slope ($D_2$), effective area ($A_{\mathrm{eff}}$), and attenuation ($\alpha$) of the fibers are reported in Table I.

The overall transmission link is 600 km with the lengths of each NZDSF span ranging between 95 and 110 km. The length of the added SMF spool ($L_{\mathrm{SMF}}$) is approximately 13 km, such that $L_{\mathrm{SMF}} D_{\mathrm{SMF}} \cong D_{\mathrm{NZDSF}}(L_{\mathrm{amp}} - 1/\alpha_{\mathrm{NZDSF}})$. To stress the nonlinear effects along this system, which is short compared to standard long-haul links, the output power of the amplifiers (and input to fiber spans) was first set to 12 dBm, and later to 13 dBm.

### C. Optical Phase Conjugator

The OPC device (Fig. 3) is based on a 67-mm-long, fiber-pigtailed, reverse-proton-exchanged waveguide fabricated on a periodically poled lithium-niobate substrate. The conjugated signal was obtained through the cascading technique in a polarization-dependent setup, although several polarization-independent schemes have already been proposed [15], [16] and demonstrated in wavelength-division-multiplexing (WDM) field-trial experiments [17]. The device is characterized by a fiber-to-fiber insertion loss of less than 3.2 dB and a 60-mm-long quasi-phase-matching section allowing for highly efficient wavelength conversion. The pump and the signal are

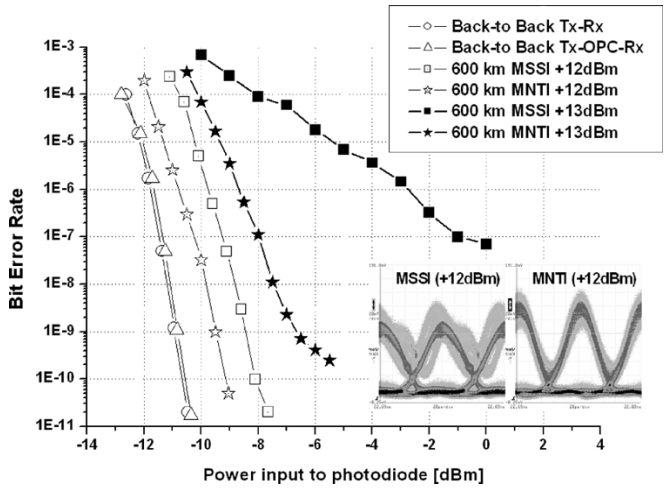


Fig. 4. BER curves versus optical power input to the photodiode. In the lower right corner, the eye diagrams obtained in the two configurations, at the same power, are reported. The one on the right (MNTI) is wide open, while the diagram on the left (MSSI) clearly shows multiple levels on both ones and zeros due to the nonlinear effects accumulated during propagation.

separately amplified, filtered for noise removal, and then input to the waveguide via a coupler, giving a net pump power input to the waveguide of about 150 mW. The OPC gives $-10$-dB conversion efficiency, measured at the device output as the ratio between signal power and converted-signal power. After the filter inserted at the waveguide output, the converted-signal power was $-2$ dBm.

## IV. Experimental Results

To compare the performance of the two configurations shown in Fig. 1, the BER curves have been measured as a function of the power input to the photodiode (Fig. 4).

The penalty introduced by the OPC setup is negligible; conversely, a significant distortion, which can be ascribed mainly to self-phase modulation (SPM) and secondarily to the intrachannel cross-phase modulation (IXPM), is introduced during propagation. BER curves after 600 km, at 12-dBm input power show error-free operation for both configurations, while maintaining a constant slope; yet, in the MNTI configuration, the transmission penalty is reduced by 1.3 dB. When the optical output power of the amplifiers is raised to 13 dBm, both BER curves show a decreased slope due to the presence of an error floor. The MSSI configuration leads to a BER floor of $\sim 10^{-7}$, while the floor level is less than $2{\cdot}10^{-10}$ for MNTI. Moreover, even at a BER level of $10^{-7}$, MNTI offers a significant 7-dBm advantage over the MSSI setup.

## V. Conclusion

The effectiveness of the MNTI-based solution proposed in [13] has been experimentally demonstrated for the first time. By simply combining a highly efficient phase conjugator and two lumped dispersion compensator modules, the simultaneous cancellation of dispersion and nonlinear effects (mainly SPM and IXPM) has been achieved. This technique is particularly interesting to upgrade "noncustomized" systems with lumped optical amplifiers and strongly asymmetrical power profiles. In principle, this approach should allow us to compensate for single-channel nonlinearities even on WDM systems, although its extension to interchannel nonlinearities is still under analysis. The only requirement would be that the signal bit rate must be sufficiently high to allow modeling the nonlinear effects as a small perturbation to the dominant dispersive effects.

## References

[1] A. Mecozzi, C. B. Clausen, and M. Shtaif, "System impact of intrachannel nonlinear effects in highly dispersed optical pulse transmission," *IEEE Photon. Technol. Lett.*, vol. 12, no. 12, pp. 1633–1635, Dec. 2000.

[2] J. P. Gordon and L. F. Mollenauer, "Phase noise in photonic communications system using linear amplifiers," *Opt. Lett.*, vol. 15, pp. 1351–1353, Dec. 1990.

[3] A. Chowdhury *et al.*, "Compensation of intrachannel nonlinearities in 40-Gb/s pseudolinear systems using optical-phase conjugation," *J. Lightw. Technol.*, vol. 23, no. 1, pp. 172–177, Jan. 2005.

[4] S. L. Jansen *et al.*, "Reduction of Gordon-Mollenauer phase noise by midlink spectral inversion," *IEEE Photon. Technol. Lett.*, vol. 17, no. 4, pp. 923–925, Apr. 2005.

[5] X. Tang and Z. Wu, "Reduction of intrachannel nonlinearity using optical phase conjugation," *IEEE Photon. Technol. Lett.*, vol. 17, no. 9, pp. 1863–1865, Sep. 2005.

[6] A. Yariv, D. Fekete, and D. M. Pepper, "Compensation for channel dispersion by nonlinear optical phase conjugation," *Opt. Lett.*, vol. 4, pp. 52–54, Feb. 1979.

[7] D. M. Pepper and A. Yariv, "Compensation for phase distortions in nonlinear media by phase conjugation," *Opt. Lett.*, vol. 5, pp. 59–60, Feb. 1980.

[8] W. Pieper *et al.*, "Nonlinearity-insensitive standard-fiber transmission based on optical-phase conjugation in a semiconductor-laser amplifier," *Electron. Lett.*, vol. 30, pp. 724–726, Apr. 1994.

[9] S. Watanabe, "Exact compensation for both chromatic dispersion and Kerr effect in a transmission fiber using optical phase conjugation," *J. Lightw. Technol.*, vol. 14, no. 3, pp. 243–248, Mar. 1996.

[10] I. Brener *et al.*, "Cancellation of all Kerr nonlinearities in long fiber spans using a LiNbO3 phase conjugator and Raman amplification," in *OFC Conf. 2000*, vol. 4, 2000, pp. 266–268.

[11] P. Minzioni, F. Alberti, and A. Schiffini, "Optimized link design for nonlinearity cancellation by optical phase conjugation," *IEEE Photon. Technol. Lett.*, vol. 16, no. 3, pp. 813–815, Mar. 2004.

[12] P. Minzioni and A. Schiffini, "Unifying theory of compensation techniques for intrachannel nonlinear effects," *Opt. Express*, vol. 13, pp. 8460–8468, Oct. 2005.

[13] P. Minzioni, F. Alberti, and A. Schiffini, "Techniques for nonlinearity cancellation into embedded links by optical phase conjugation," *J. Lightw. Technol.*, vol. 23, no. 8, pp. 2364–2370, Aug. 2005.

[14] P. Minzioni *et al.*, "Efficient nonlinearity cancellation through optical phase conjugation into an embedded link with asymmetrical power profiles," in *OFC Conf. 2006*, Anaheim, CA, Paper OThA7.

[15] M. H. Chou, K. R. Parameswaran, M. M. Fejer, and I. Brener, "Optical signal processing and switching with second-order nonlinearities in waveguides," *IEICE Trans. Electron.*, vol. E83-C, pp. 869–874, Jun. 2000.

[16] I. Cristiani, V. Degiorgio, L. Socci, F. Carbone, and M. Romagnoli, "Polarization-insensitive wavelength conversion in a lithium niobate waveguide by the cascading technique," *IEEE Photon. Technol. Lett.*, vol. 14, no. 5, pp. 669–671, May 2002.

[17] D. Caccioli *et al.*, "Field demonstration of in-line all-optical wavelength conversion in a WDM dispersion managed 40-Gb/s link," *IEEE J. Sel. Topics Quantum Electron.*, vol. 10, no. 2, pp. 356–362, Mar./Apr. 2004.